Article:
Stark, H., Wolf, J., Albersmeier, A. et al. (7 more authors) (2017) Oxidative Stickland reactions in an obligate aerobic organism – amino acid catabolism in the Crenarchaeon Sulfolobus solfataricus. The FEBS Journal, 284 (13). pp. 2078-2095. ISSN 1742-464X

https://doi.org/10.1111/febs.14105

Oxidative Stickland reactions in an obligate aerobic organism — amino acid catabolism in the Crenarchaeon *Sulfolobus solfataricus*

Helge Stark[1,*], Jacqueline Wolf[1,*], Andreas Albersmeier[2], Trong K. Pham[3], Julia D. Hofmann[1], Bettina Siebers[4], Jörn Kalinowski[2], Phillip C. Wright[3], Meina Neumann-Schaal[1,†] and Dietmar Schomburg[1]

[1]Department of Bioinformatics and Biochemistry, Technische Universität Braunschweig, 38106 Braunschweig, Germany

[2]Center for Biotechnology – CeBiTec, Universität Bielefeld, 33615 Bielefeld, Germany

[3]Departement of Chemical and Biological Engineering, ChELSI Institute, University of Sheffield, S1 3JD, Sheffield, UK

[4]Molecular Enzyme Technology and Biochemistry, Biofilm Centre, Universität Duisburg-Essen, 45141 Essen, Germany

*These authors contributed equally to this work

Article type : Original Article

Running title: Stickland reactions in *Sulfolobus solfataricus*

Conflict of interest: The authors declare that they have no conflict of interest.

Keywords: *Sulfolobus*; systems biology; amino acid degradation; Stickland reactions; biological model

Data Accessibility: The SEEK platform (https://seek.sysmo-db.org/studies/169)

Abbreviations:

CoA	–	coenzyme A
CDW	–	cell dry weight
FBA	–	flux-balance analysis
GAM	–	growth-associated maintenance energy

This article has been accepted for publication and undergone full peer review but has not been through the copyediting, typesetting, pagination and proofreading process, which may lead to differences between this version and the Version of Record. Please cite this article as doi: 10.1111/febs.14105

MSTFA – *N*-Methyl-*N*-(trimethylsilyl)trifluoroacetamide
NGAM – non-growth-associated maintenance energy
OD – optical density

† **Corresponding author:**
E-Mail: m.neumann-schaal@tu-braunschweig.de
Phone: +49-531-391 55205

Abstract

The thermoacidophilic Crenarchaeon *Sulfolobus solfataricus* is a model organism for archaeal adaptation to extreme environments and renowned for its ability to degrade a broad variety of substrates. It has been well characterised concerning the utilisation of numerous carbohydrates as carbon source. However, its amino acid metabolism, especially the degradation of single amino acids, is not as well understood.

In this work, we performed metabolic modelling as well as metabolome, transcriptome and proteome analysis on cells grown on caseinhydrolysate as carbon source in order to draw a comprehensive picture of amino acid metabolism in *S. solfataricus* P2. We found that 10 out of 16 detectable amino acids are imported from the growth medium. Overall, uptake of glutamate, methionine, leucine, phenylalanine and isoleucine was the highest of all observed amino acids. Our simulations predict an incomplete degradation of leucine and tyrosine to organic acids and, in accordance with this, we detected the export of branched-chain and aromatic organic acids as well as amino acids, ammonium and trehalose into the culture supernatants. The branched-chain amino acids as well as phenylalanine and tyrosine are degraded to organic acids via oxidative Stickland reactions. Such reactions are known for prokaryotes capable of anaerobic growth, but so far has never been observed in an obligate aerobe. Also, 3-methyl-2-butenoate and 2-methyl-2-butenoate are for the first time found as products of modified Stickland reactions for the degradation of branched-chain amino acids. This work presents the first detailed description of branched-chain and aromatic amino acid catabolism in *S. solfataricus.*

Introduction

Archaea are the predominant life-form in various extreme environments. The obligate aerobic Crenarchaeon *Sulfolobus solfataricus*, growing optimally at 80 °C and pH 3.5, was originally isolated from hot acidic springs at Pisciarelli Solfatara in Italy [1,2]. Nowadays, *S. solfataricus* is considered to be

a model organism for archaeal adaptation to extreme environments and changing nutrient conditions [2–4]. Its carbohydrate metabolism has been analysed in a number of papers and ranges from alcohols and monosaccharides up to macromolecules like cellulose [3,5–13]. However, there is only limited information available about the organism's amino acid metabolism, especially concerning the uptake and degradation of individual amino acids, which could be mainly attributed to its inability to grow on individual amino acids as sole carbon source [7,14]. This is quite surprising considering that many species of the genus *Sulfolobus* were originally isolated in amino acid rich complex media [1,2,15]. Understanding the organism's amino acid catabolism will facilitate the creation of defined, amino acid-containing media. It will also help in reducing the production of unwanted by-products from amino acids that can interfere with the organism's growth behaviour such as pyroglutamate and organic acids, which has been reported for hyperthermophile archaea [16,17].

So far, *S. solfataricus* is known to be prototrophic for all its amino acids and in accordance to this biosynthesis pathways for all proteinogenic amino acids have been postulated from the genome sequence [18]. Also, it was shown that *S. solfataricus* reacts quite sensitive to the presence and concentration of single amino acids. While glutamate and aspartate can enhance growth of *S. solfataricus* [14], high concentrations of glutamate have an adverse effect, most likely due to the spontaneous formation of growth inhibiting pyroglutamate from glutamate at low pH and temperatures above 78 °C [19,20]. In anaerobic archaea, amino acids have been proposed to be degraded via a series of oxidative Stickland reactions which lead to the production of organic acids [16]. Originally, Stickland reactions have been described for bacteria capable of anaerobic growth. In these organisms a reductive branch transfers electrons gained from the simultaneous oxidation of other amino acids onto acceptor amino acids [21–23]. In archaea however, only the oxidative branch of Stickland reactions has been observed. The archaeal enzymes catalysing these reactions have been shown to produce 2-ketoacids derived from valine, leucine, isoleucine, phenylalanine and glutamate *in vitro* [17,24] and *Thermococcus kodakarensis* was shown to export 2-ketoacids when supplied with extracellular amino acids [16].

To elucidate the uptake and utilisation of amino acids in *S. solfataricus* P2 we cultivated the organism on medium containing caseinhydrolysate as sole carbon and nitrogen source and compared it to growth on glucose minimal medium. The observed growth and uptake rates were integrated into an updated version of our previously published genome-scale metabolic model of *S. solfataricus* P2 [25] which predicts incomplete degradation of leucine and tyrosine to organic acids. In order to monitor changes between the two growth conditions on a global level we further used metabolomics, transcriptomics and proteomics. A time-resolved amino acid uptake pattern revealed that 10 out of the 16 detectable amino acids were taken up by the organism whereas 4 amino acids, trehalose and several organic acids were exported. Ultimately, we are able to demonstrate that in addition to known degradation pathways *S. solfataricus* P2 also

actively degrades branched-chain and aromatic amino acids via oxidative Stickland reactions. The final products of these reactions are branched-chain or aromatic organic acids accumulating in the culture supernatant. This is the first description of amino acid degradation via oxidative Stickland reactions in an obligate aerobe. Additionally two of the detected branched-chain organic acids, namely 3-methyl-2-butenoate and 2-methyl-2-butenoate, have neither been observed nor yet linked to oxidative Stickland reactions. These branched-chain organic acids are generated by a slightly varied Stickland pathway that comprises an additional oxidation reaction of the carboxyl-CoA intermediates.

Results and Discussion

S. solfataricus P2 was cultivated on either defined medium containing 1 % caseinhydrolysate (w/v) as sole carbon and nitrogen source or on minimal medium containing **0.44 %** glucose (w/v) as sole carbon source and **0**.13 % ammonium sulfate as sole nitrogen source. The glucose culture served as a reference condition in this work. Non-inoculated medium containing caseinhydrolysate was used as control to investigate amino acid stability under cultivation conditions. All cultivations were performed at 78 °C.

With caseinhydrolysate as carbon source *S. solfataricus* reached a cell dry weight of 0.44 $g \cdot l^{-1}$ and showed a maximum growth rate of 0.03 h^{-1} within 100 hours of cultivation compared to the glucose reference culture, which showed a maximum growth rate of 0.045 h^{-1} (Figure 1). The cultures growing on caseinhydrolysate entered the logarithmic growth phase after 30 hours and the stationary growth phase after 90 hours of cultivation. The observed growth behaviour clearly indicates that *S. solfataricus* uses glucose more efficiently as carbon source than amino acids. Recently it was shown, that 47 % of the carbon from glucose is incorporated into the biomass, whereas the rest is completely oxidized to carbon dioxide [10]. In contrast, as we demonstrate in this work, only a few amino acids are efficiently consumed from the media. Further, the majority of these were incompletely oxidized to short chain organic acids and secreted (see below). Thus, this carbon loss together with the limited uptake of amino acids mainly contributes to the lower biomass yield during growth on caseinhydrolysate.

Preferential uptake of glutamate, methionine, leucine, phenylalanine and isoleucine

In order to analyse the relative consumption of individual amino acids, samples were taken at different time points from cultures grown on caseinhydrolysate and the supernatants were analysed via GC-MS. The uptake profile for 16 detectable amino acids as well as the formation of pyroglutamate is illustrated in Figure 2. A differential preference for certain amino acids was observed, i. e. a total uptake of 30 – 50 % for glutamate, methionine, leucine, phenylalanine and isoleucine followed by 15 – 20 % for threonine, alanine, aspartate, glycine and tyrosine. This shows that the organism prefers glutamate, leucine and isoleucine over the remaining amino acids. During the first 21 hours, glutamate is the only amino acid to

be taken up (initial concentration: 5.6 mM). Also, the consumption of glutamate is the highest of all amino acids (glutamate remaining after 101 h: 1.9 mM). As the heat-induced formation of pyroglutamate from glutamate is known [19,20] a parallel cell-free experiment was done and the formation of pyroglutamate determined. Pyroglutamate was formed in both the control cultures as well as the inoculated samples. In the inoculated cultures pyroglutamate concentrations peaked at about 1.5 mM at 66 hours of cultivation and fell back to about 0.9 mM at the end of cultivation. Methionine and leucine are only imported after 24 h and isoleucine and phenylalanine after 66 – 77 h.

When cells entered the stationary phase none of the amino acids had been completely consumed. Hence, neither C- nor N-limitation can be responsible for the impaired growth on caseinhydrolysate. The pH was constantly monitored and maintained between 3.5 and 4.0 as well. The observed uptake of pyroglutamate could possibly contribute to the observed growth impairment since pyroglutamate has been shown to negatively affect growth of thermophilic archaea [14,20] and, in this regard, it has been discussed to act as protonophore which interferes with respiration and pH homeostasis [26,27]. However, the pyroglutamate concentrations in the inoculated cultures were far below the reported value of 15.5 mM required to interrupt growth of *S. solfataricus* P2 [28]. Interestingly, several small organic acids (e.g. 2- and 3-Methylbutanoate, 2-Methyl-2-butenoate; see below) have been detected in the culture supernatants only during growth on caseinhydrolysate, which could also contribute to the observed early entrance into the stationary growth phase. Due to the low extracellular pH, these acids become protonated and could then enter the cell by diffusion. As *S. solfataricus* maintained an internal near neutral pH these acids immediately dissociate. Thus, such 'uncouplers' mediate the net uniport of protons and uncouple proton transport from cellular processes (e.g. ATP synthase). If proton extrusion proceeds not fast enough, this process would finally lead to an overacidification of the cytosol [26,29,30].

Secretion of organic acids, ammonium, amino acids and trehalose

The supernatants of cultures grown on caseinhydrolysate were analysed via GC-MS in order to screen the growth medium for any metabolites exported by *S. solfataricus*. An accumulation of several organic acids as well as ammonium, amino acids, pipecolate and trehalose was observed in the culture supernatants.

We detected the aromatic organic acids 2-hydroxyphenylacetate and 4-hydroxyphenylacetate as well as the branched-chain organic acids isovalerate, 2-methylbutanoate, isobutanoate, 3-methyl-2-butenoate, 2-methyl-2-butenoate and of 3-hydroxyisovalerate in the culture supernatants. The branched-chain organic acids accumulated over the course of cultivation (Figure 3) and are linked to the degradation of the amino acids leucine, isoleucine and valine (Figure 4) whereas the aromatic organic acids are linked to the degradation of phenylalanine and tyrosine (Figure 5). Except 3-hydroxyisovalerate all other branched-

chain organic acids were already exported at an early stage of growth and appeared in the supernatants after 21 hours of cultivation. These compounds were found to be highly abundant in the culture supernatants during the whole cultivation period. So far, the organic acids isovalerate, 2-methylbutanoate and isobutanoate have only been described as product of Stickland reactions in anaerobic organisms capable of amino acid degradation [16,22]. This was surprising, considering that *S. solfataricus* is an obligate aerobe organism [31]. Incomplete oxidation of amino acids has not yet been reported for this organism. In the following sections, the data acquired in this work was used to elucidate the formation of the detected organic acids in *S. solfataricus* P2.

The presence of extracellular ammonium suggests that export of ammonium is the primary mode for disposal of excess nitrogen in *S. solfataricus*. In addition to the export of organic acids and ammonium, we observed export of pipecolate and of the nitrogen-rich amino acids lysine, histidine and arginine. The formation of these compounds requires energy investment and leads to a loss of carbon. Such a behaviour indicates overflow metabolism, which is reported for many organisms cultivated in nutrient-rich media [32]. Pipecolate is also known as a product of lysine degradation, however, to date no pathway for lysine degradation has been reported for *S. solfataricus*.

Trehalose starts to accumulate extracellularly up to 24-fold during the stationary growth phase even though intracellular trehalose concentrations did not change significantly. This compound is known to serve as a compatible solute in response to osmotic stress and as storage carbohydrate similar to glycogen [33]. Compared to growth on glucose, key enzymes for gluconeogenesis (Sso0527 and Sso0528) are slightly more abundant (up to 2.6-fold in proteome) whereas key enzymes for glucose degradation (Sso3003, Sso3042) are less abundant in cells grown on caseinhydrolysate (down to 0.4-fold in proteome; Table 1). An increased flux through enzymes of gluconeogenesis could lead to an increased production of trehalose which, due to overflow metabolism, is exported out of the cell.

Branched-chain amino acids are incompletely degraded to organic acids via oxidative Stickland reactions

Metabolome analysis allowed the reconstruction of degradation pathways for all three branched-chain amino acids (Figure 4). According to our metabolic model, complete degradation pathways are present for isoleucine (reactions 10–18) and valine (reactions 21–27, 16–18) whereas leucine can only be degraded to mevalonate (reactions 1–6) which is further used in isoprenoid biosynthesis. The first three steps of common pathways for degradation of branched-chain amino acids are identical for all three amino acids (reactions 1–3 / 11–13 / 22–24) and catalysed by the same set of enzymes. Among the enzymes catalysing these reactions the 2-ketoacid:ferredoxin oxidoreductase responsible for converting 2-ketoacids to their corresponding CoA-derivatives (reaction 2 / 12 / 23), namely 2-ketoisovalerate:ferredoxin oxidoreductase (Sso2756–Sso2758, Sso11071), is significantly up-regulated up to 17-fold (Table 1). The remaining steps

in branched-chain amino acid degradation are different for leucine, isoleucine and valine although some enzymes are shared in these pathways as well (Figure 4). 3-Hydroxy-3-methylglutaryl-CoA (reaction 5) acts as a direct precursor of mevalonate, a key intermediate in isoprenoid biosynthesis [34]. No homologue of 3-hydroxy-3-methylglutaryl-CoA lyase (EC 4.1.3.4) required for subsequent leucine degradation was found. For the remaining enzymes involved in isoleucine or valine degradation (reactions 14–19 / 25–28) enzyme candidates are presented.

Most importantly, all of the extracellularly detected branched-chain organic acids (Figure 3) can be produced in *S. solfataricus* P2 via a series of oxidative Stickland reactions [16,23] from branched-chain amino acids. The term 'Stickland reactions' typically comprises fermentation pathways in which amino acids are degraded in a pairwise manner with one amino acid acting as electron donor (oxidative reactions) while the other amino acid acts as electron acceptor (reductive reactions) [22]. However, only oxidative Stickland reactions have so far been observed in archaea, all of which are capable of anaerobic growth [16,17,24]. In *S. solfataricus*, most of the relevant reactions for the oxidative Stickland reactions of branched chain amino acids are shared with common degradation pathways for aerobic branched-chain amino acid degradation (reactions 1–3 / 11–13 / 22–24) and follow the scheme proposed by Yokooji *et al.* [16], which suggests subsequent activity of the enzymes amino acid aminotransferase, 2-oxoacid:ferredoxin oxidoreductase and ADP-forming acetate-CoA ligase. Several 2-oxoacid:ferredoxin oxidoreductases (EC 1.2.7.-) are characteristic for oxidative Stickland reactions and are highly conserved even between archaea and bacteria [22,35–37]. Their limited presence in (facultative) anaerobes is probably due to the oxygen sensitivity of this type of oxidoreductases [38,39]. In contrast, however, the 2-oxoacid:ferredoxin oxidoreductase from *Sulfolobus tokodaii* has been shown to be oxygen resistant [38]. The activity of oxidoreductases in *S. solfataricus* demonstrated by the presence of organic acids in this work suggests that the oxygen resistance of this group of enzymes is common to the genus *Sulfolobus*. The final enzyme required for the formation of the branched-chain organic acids from corresponding CoA-derivatives (reactions 7, 8, 10, 20, 21, 29) is an ADP-dependent acetate-CoA ligase that has previously been isolated from archaea (EC 6.2.1.13) and which is specifically capable of catalysing the formation of ATP and organic acids [16,24,40,41]. The respective enzyme was shown to produce the branched-chain organic acids isovalerate and isobutanoate in *Pyrococcus furiosus* [42], 2-oxoglutarate in *Thermococcus kodakarensis* [16] as well as isobutanoate and phenylacetate in *Pyrobaculum aerophilum* [41]. Similar to other archaea acetate-CoA ligase is a fusion protein of two subunits in *S. solfataricus* [41]. The production of this protein on locus *Sso1806* was proven by transcriptome and proteome analysis and it is slightly increased in cells grown on caseinhydrolysate (2.6-fold in proteome). We therefore postulate that acetate-CoA ligase is responsible for the production of branched-chain organic acids in *S. solfataricus.*

To our knowledge this work is the first report of oxidative Stickland reactions in an obligate aerobic organism. While isovalerate, 2-methylbutanoate, isobutanoate and phenylacetate have already been described as products of oxidative Stickland reactions in anaerobic and facultative anaerobic organisms, we were surprised to also identify the metabolites 3-methyl-2-butenoate and 2-methyl-2-butenoate in supernatants of cells grown on caseinhydrolysate. This indicates that the acetate-CoA ligase responsible for the generation of the mentioned carboxylic acids is also able to accept the reduced CoA-derivatives generated by isovaleryl-CoA dehydrogenase (reaction 8 / 21) and enoyl-CoA hydratase (reaction 10) as substrates. Both, 2-methyl-2-butenoate and 3-methyl-2-butenoate, can be reported as newfound products of oxidative Stickland reactions.

Aromatic amino acids are catabolised to organic acids via oxidative Stickland reactions as well

Degradation of the aromatic amino acids phenylalanine and tyrosine showed remarkable similarities to the Stickland-like degradation of branched-chain amino acids.

Not only branched-chain organic acids but also the corresponding aromatic organic acids 4-hydroxyphenylacetate and 2-hydroxyphenylacetate were detected in the intracellular and extracellular space of cells grown on caseinhydrolysate (Figure 5). In contrast to the Stickland degradation of branched-chain amino acids another class of ferredoxin-oxidoreductases (EC 1.2.7.8) [24,44] is responsible for the formation of aromatic CoA-intermediates (reactions 11, 14). The transcription of two genes (*Sso2067* & *Sso2069*) encoding for both subunits of this protein was found to be significantly increased in medium containing caseinhydrolysate. Presumably, the acetate-CoA ligase homologue (Sso1806) is again responsible for the formation of phenylacetate (as was shown for *P. aerophilum* [41]) and 4-hydroxyphenylacetate from their respective CoA-derivatives (reactions 11, 14) since both metabolites as well as phenylacetyl-CoA were significantly more abundant in cells grown on caseinhydrolysate. Phenylacetate, which could only be detected in cells grown on caseinhydrolysate (Table 2), can be further metabolised to 2-hydroxyphenylacetate (and also to 4-hydroxyphenylacetate) via action of monooxygenases. The best relevant candidate for a 4-hydroxyphenylacetate-3-hydroxylase (Sso2053) shares high sequence similarity to the enzyme from *Pseudomonas putida* (identity: 37 %, e-value: $4 \cdot 10^{-90}$) which was shown to exhibit a broad substrate specificity including phenylacetate [45]. All in all, the Stickland-like incomplete oxidation of aromatic amino acids observed in this work has not yet been reported for obligate aerobic organisms.

We also obtained the first experimental proof that the bacterial phenylalanine degradation pathway

proposed by Teufel *et al.* [46] is also active in an archaeon (Figure 5, reactions 1–10). For archaea, key enzymes of this pathway have so far only been predicted from computational genome analysis for members of the Halobacteria [47]. Since several of the intermediates (phenylacetyl-CoA, 3-oxo-5,6-dehydrosuberyl-CoA semialdehyde, 2,3-dehydroadipyl-CoA) of this pathway were detected in the metabolome, it is hereby confirmed to be present in *S. solfataricus*. In *S. solfataricus*, the homology to known, characterised enzymes of the bacterial phenylalanine degradation pathway is low. Still, all predicted loci in this work were found to be actively transcribed on a low level in all examined cultures. The high abundance of the hydroxyphenylacetate isomers in the culture supernatants and of phenylacetate and phenylacetyl-CoA intracellularly correspond to the comparably low transcription levels of the enzymes involved in the bacterial phenylalanine degradation pathway. Furthermore, a large number of intermediates of this **pathway** could not be detected. Hence, we postulate that the formation of phenylacetate and hydroxyphenylacetate isomers is an important feature of aromatic amino acid metabolism in *S. solfataricus* P2.

Sulfolobaceae are the only Crenarchaeota with proven oxidative Stickland reactions in an aerobic environment

In order to evaluate the distribution of enzymes involved in oxidative Stickland reactions among archaea we queried the database BRENDA [48] for literature on the respective enzymes. We found that the ferredoxin oxidoreductases EC 1.2.7.7 and EC 1.2.7.8 are well explored in Euryarchaeota as there is literature on at least 11 organisms from the genuses *Archaeoglobus*, *Haloarcula*, *Methanococcus*, *Methanothermobacter*, *Pyrococcus* and *Thermococcus* on these enzymes. Among these organisms the presence of ATP-forming acetate-CoA ligase (EC 6.2.1.13) was also reported for *Haloarcula marismortui* [41], *Pyrococcus furiosus* [24,42,49] and *Thermococcus kodakarensis* [40]. For Crenarchaeota there is only literature available on acetate-CoA ligase from *Pyrobaculum aerophilum* and *Pyrobaculum islandicum*. It seems that the presence of oxidative Stickland reactions in Euryarchaeota is a known phenomenon but has not yet been a primary subject of research in Crenarchaeota.

We also performed BLAST searches with the protein sequences of EC 1.2.7.7, EC 1.2.7.8 and EC 6.2.1.13 from the Euryarchaeon *P. furiosus* and the Crenarchaeon *S. solfataricus* against all published genomes of archaea using the NCBI pBLAST [50] and the BLOSUM62 similarity matrix. We found that 179 species of archaea (including Euryarchaea and Crenarchaea) exhibited high sequence similarities to at least one queried acetate-CoA ligase and one queried ferredoxin oxidoreductase (https://seek.sysmo-db.org/data_files/1644). Thus, the genes which enable archaea to degrade amino acids using oxidative Stickland reactions are widely distributed in this domain of life. Obligate aerobes are generally uncommon among archaea [51] and only five of the 179 candidates have been described as such, all of which belong to the family Sulfolobaceae and thus are Crenarchaeota: *Metallosphaera cuprina*,

Metallosphaera sedula, *Sulfolobus islandicus*, *Sulfolobus solfataricus* and *Sulfolobus tokodaii*. The capability to degrade amino acids using oxidative Stickland reactions seems to be a common feature in archaea, however, the only obligate aerobe prokaryotes deploying this strategy of amino acid degradation presumably will be members of the family Sulfolobaceae.

Amino acid degradation via oxidative Stickland reactions in the metabolic model

We used an updated version of our previously published genome-scale metabolic model of *S. solfataricus* P2 [25] to predict intracellular metabolite fluxes for growth on caseinhydrolysate as sole carbon source. This model was also used to identify gene candidates for the enzymes required in the reconstruction of amino acid metabolism in the organism. The pathways specific for branched-chain and aromatic amino acid degradation derived by combination of experimental and bioinformatics methods are shown in Figure 4 and Figure 5. The updated version of our metabolic model (supplied with this publication and available on the SEEK platform [52] (https://seek.sysmo-db.org/models/231) is comprised of 1035 reactions and 607 genes. Experimental data obtained in this study were used to improve the metabolic model: a caseinhydrolysate-specific biomass reaction based on the specific biomass composition (see Materials and Methods section) was added to the model, growth rates were used to fit energy maintenance parameters and substrate uptake rates (Table 3) were used to define the caseinhydrolysate-specific scenarios (see Materials & Methods section).

For the intracellular degradation of individual amino acids some common pathways can be postulated from the genome sequence. The first steps of glutamate and aspartate degradation in *S. solfataricus* are probably catalysed by glutamate dehydrogenase [53,54] and aspartate transaminase [55]. No information, apart from bioinformational predictions, is available for the degradation of other amino acids in this organism.

In our simulations all ten amino acids that were experimentally shown to be taken up by *S. solfataricus* P2 (Table 3) are also imported by the metabolic model. Glutamate is predicted to be the main carbon source, followed by leucine which can not be completely oxidised to CO_2 but instead is used for the production and export of organic acids in all scenarios. Within the model the simulated degradation of the branched-chain amino acids leucine, isoleucine and valine as well as from the aromatic amino acids phenylalanine and tyrosine can lead to the production and export of organic acids due to the utilisation of oxidative Stickland reactions (Table 3). In the freely optimised scenario the amino acids leucine and tyrosine are already being degraded to organic acids via a series of oxidative Stickland reactions [23] (Figure 4, reactions 1–3, 8 / Figure 5, 12–14) since no enzymes for alternative degradation pathways could be annotated from the genome sequence. In addition to organic acids derived from leucine and tyrosine, in the forced-Stickland scenario the amino acids isoleucine and phenylalanine are also degraded

via oxidative Stickland reactions since common pathways yielding succinyl-CoA and acetyl-CoA (Figure 4, reactions 11–19 / Figure 5, reactions 1–10) have been deactivated (Table 3). Compared to the common degradation pathways that can yield biomass precursors the production and export of organic acids is equivalent to a loss of carbon. In the forced-Stickland scenario 15.9 % of all imported carbon is exported in the form of organic acids compared to 7.7% in the 'free' scenario. The metabolic model predicts a slightly lower biomass flux for the forced-Stickland scenario (0.026 h^{-1}) compared to the freely optimised scenario (0.030 h^{-1}). The slightly lower biomass flux in the 'forced' scenario is a direct consequence of the mentioned carbon loss, since the objective function for our simulations is optimal biomass production and therefore dependent on optimal usage of carbon. This, however, must not be true *in vivo*, since all amino acids are still present at the end of cultivation (Figure 2) and thus carbon is no growth-limiting factor. Apart from this, the degradation via Stickland reactions contributes to the ATP production in our metabolic model (Table 4) which explains why this degradation strategy can be used by *S. solfataricus* when growing in amino acid rich medium. Furthermore, the utilisation of Stickland reactions explains the inability of *S. solfataricus* to grow on these amino acids as sole carbon source**.**

Global changes in metabolome, transcriptome and proteome compared to glucose reference culture

For untargeted metabolome, transcriptome and proteome analysis, we took samples from all cultures during the logarithmic growth phase. GC-MS and HPLC-MS analysis were used to monitor changes in the intracellular metabolome of *S. solfataricus* P2 grown on caseinhydrolysate compared to the glucose reference (Table 5). We were able to detect 14 amino acids, all of which are more abundant on or only present in cells grown on caseinhydrolysate including some amino acids not significantly imported from the medium (Figure 6, Table 2). Likewise, several metabolites linked to common amino acid catabolism (Figure 6) are significantly increased compared to the glucose reference. This is also true for CoA-derivatives and organic acids linked to oxidative Stickland reactions (Figure 4, Figure 5). The TCA cycle intermediates fumarate, succinate and malate are also significantly increased in cells grown on caseinhydrolysate whereas succinyl-CoA is significantly reduced. The classical degradation pathways of branched chain amino acids and also of phenylalanine would result in the formation of succinyl- and acetyl-CoA. However, the decreased abundance of succinyl-CoA and the unchanged levels of acetyl-CoA indicate a minor importance of classical degradation routes and strongly suggests that the amino acid degradation via Stickland oxidation is active in *S. solfataricus*.

Also significantly reduced are sugars and sugar derivatives (e.g. glucose, erythronate, methyl-α-D-glucopyranoside) as well as the isoprenoid biosynthesis intermediates 3-hydroxy-3-methylglutaryl-CoA and glycerol-1-phosphate. The decreased abundance of sugars and their derivatives correlates with the decreased intracellular glucose levels. Isoprenoids on the other hand are required for lipid biosynthesis in

archaea [56] thus the decreased levels of intermediates of isoprenoid biosynthesis (3-hydroxy-3-methylglutaryl-CoA and glycerol-1-phosphate) are probably a result of the decreased growth rate. Furthermore, we observed significant amounts of several N-containing compatible solutes such as the polyamines norspermidine and spermidine solely in cells grown on caseinhydrolysate. In contrast to the secretion of amino acids and ammonium to dispose excess nitrogen, these compounds may serve as intermediate storage for intracellular nitrogen.

We also used transcriptomics and proteomics to monitor the changes in relative abundance of transcripts and proteins for growth on caseinhydrolysate (Table 5). Most of the differentially expressed genes and differentially produced proteins with annotated function can be assigned to either transport processes, amino acid degradation or amino acid biosynthesis pathways. Of the 50 most differentially expressed genes and differentially produced proteins with known or postulated annotation (Table 1) 13 are linked to transport processes, eight to amino acid degradation (all up-regulated) and seven to amino acid biosynthesis (all down-regulated). The remaining loci code for a variety of proteins including molybdopterin-binding subunits of uncharacterised oxidoreductases, alternative quinol oxidase subunits, heterodisulfide reductase and isocitrate lyase.

The up-regulated genes encoding for transport proteins are mainly comprised of permeases, whereas the down-regulated genes encoding for transporters include two carbohydrate transporters, an ammonium transporter and a metal permease. Up-regulated genes involved in amino acid degradation are mainly required for the degradation of glutamate and branched-chain amino acids, such as glutamate dehydrogenase encoded on *Sso2044* and *Sso1907* (Table 1). We assume that glutamate degradation mainly occurs via glutamate dehydrogenase. Additionally, increased levels of 2-hydroxyglutarate, a metabolite involved in another degradation pathway for glutamate, were detected in cells grown on caseinhydrolysate. The degradation pathway via 2-hydroxyglutarate is mainly known from fermenting bacteria [57] but is also present in *S. solfataricus* P2 up to the intermediate acetyl-CoA entering the TCA cycle. Overall, the data demonstrates several key characteristics which illustrate the metabolic adaptation of *S. solfataricus* in response to growth on caseinhydrolysate. In particular it indicates a minor importance of the classical amino acid degradation pathways and suggests that oxidative Stickland reactions are active in this organism instead.

Concluding remarks

In this work we describe the global changes occurring in cells of *S. solfataricus* P2 during growth on caseinhydrolysate and present a comprehensive overview of the organism's amino acid metabolism. This includes the incomplete degradation of branched-chain and aromatic amino acids via oxidative Stickland reactions. We also present Stickland-like reactions that yield new products not yet linked to Stickland

oxidation. This is the first report of this type of reactions occurring in an obligate aerobic organism. Further, the use of oxidative Stickland reactions for degradation of several amino acids also explains the inability of *S. solfataricus* to grow on these amino acids as sole carbon source [7], as this reaction only provides ATP but no biomass precursors. The changes observed show that a small number of enzymes is sufficient to catalyse these reactions for a broad variety of amino acids, demonstrating the organism's versatility in response to environmental changes. We further confirm that the common bacterial pathway for aerobic phenylalanine degradation proposed by Teufel *et al.* [46] is also valid in archaea. These results will contribute to the understanding of archaeal amino acid metabolism, especially in the phylum Crenarchaeota.

Materials and Methods

Strain and cultivation conditions

Sulfolobus solfataricus P2 [2] was grown at 78 °C, pH 3.5 and 160 rpm (Thermotron, Infors AG, Switzerland) in defined minimal medium described by Brock et al. [15]. For growth on amino acids the medium lacks $(NH_4)_2SO_4$ and contained 10 $g \cdot l^{-1}$ caseinhydrolysate (Carl Roth GmbH, Karlsruhe, Germany) as sole carbon and nitrogen source. The composition of the lot used in this work was published previously [58]. The medium for the reference cultures contained 4.4 $g \cdot l^{-1}$ D-glucose and 1.3 $g \cdot l^{-1}$ $(NH_4)_2SO_4$ as nitrogen source. Long neck flasks (1000 ml or 500 ml, medium volume 1/5) were inoculated with glucose adapted glycerol stocks (OD_{600}: 10), prepared as described previously [59], to an initial optical density of approximately 0.03. If necessary (pH > 4.0) the pH of growing cultures was adjusted to 3.2–3.5 using 0.5 M H_2SO_4. For growth on amino acids, additional control cultures were prepared, containing either no caseinhydrolysate or no cell material. To analyse the depletion of individual amino acids during growth of *S. solfataricus* 1 ml samples were withdrawn in regular intervals from the cultivations as well as from the non-inoculated control (for testing of amino acid stability). Cells were harvested by centrifugation (20,000 x g; 5 min, 20 °C) and supernatants were stored at -20 °C until further processing. Cell growth was monitored photometrically, following the increase in optical density at 600 nm. Biomass composition was determined as described previously [10] and is available on the SEEK platform (https://seek.sysmo-db.org/data_files/1586). All samples analysed by the different '*omics'* platforms originate from the same biological replicates. For comparative '*omics'* analyses all cells were harvested in the late exponential growth phase (glucose at approx. 80 h, caseinhydrolysate at approx. 66 h). Cell harvest and sample processing was done following the protocol published by Wolf *et al.* [10].

GC-MS based analysis of intra- and extracellular compounds

Intracellular metabolites and supernatants for analysis of amino acid depletion were extracted, analysed and resulting data were processed and statistically analysed as described earlier [10].

Secretion of short chain organic acids was monitored by extraction, analysis and data processing procedures as described earlier [58]. For calculation of the absolute concentrations calibration curves ranging from 4-2000 µM for each compound were measured.

Quantification of glutamate and pyroglutamate

To circumvent the spontaneous degradation of glutamate to pyroglutamate during derivatisation and subsequent GC-MS analysis [60], glutamate was quantified by HPLC-FLD as described previously with some minor modifications [61]. The method was shortened to focus on glutamate detection. 10 min of an isocratic flow of 100 % with solvent A (0.02 M sodium acetate, pH 6.5), were followed by a gradient of solvent B (acetonitrile; 0-100 %) over 4 minutes. Finally, subsequent washing with 100 % B for 2 min was applied.

Pyroglutamate formed during cultivation was analysed after its conversion back to glutamate following the protocol described by Macpherson and Slater [62] and quantified in comparison to non-treated samples.

Extraction and analysis of intracellular CoA-derivatives

CoA-derivatives were extracted and analysed as described earlier [10]. Following data processing [10] each sample was normalised to its average peak area, excluding those CoA-intermediates in the average value that were found only in either test (caseinhydrolysate) or reference (D-glucose) condition. Statistically significant altered metabolite abundances were determined with the non-parametric Kruskal-Wallis test as described previously [10].

RNA isolation, sequencing and data analysis

RNA was isolated for all replicates using Trizol (ThermoFisher, Waltham, USA) as described earlier [63] and afterwards treated with RNase-free DNase (Qiagen). Depletion of ribosomal RNA and preparation of sequencing libraries was performed as previously described [10]. Libraries were sequenced on a HiSeq1500 instrument (Illumina) in rapid mode with a read length of 2x25nt.

Processing of raw data was performed as described elsewhere [10]. For calculation of the *reads per kilobase of gene per million reads* (RPKM) values only reads mapping to coding sequences were considered for the number of total reads. Ratios of the average RPKM values for the three replicates in both conditions were built. These ratios were shifted in order to get a median ratio of 1. For determination

of regulated genes statistical analysis was performed using DeSeq [64].

Protein extraction, iTRAQ labelling, mass spectrometry and data analysis

Protein extraction, labelling and mass spectrometry was performed as described previously [10] with the following modifications. Samples were labelled with iTRAQ 8-plex reagents as follows (6 reagents used): 113, 114 and 115 were used for cells grown on caseinhydrolysate whilst 116, 117 and 118 were used for cells grown on D-glucose (and used as control). The replicates were evaluated using dendrogram and principle component analysis (based on iTRAQ ions' intensities). There was a clear clustering and distinction between biological replicates, indicating similarity between replicates and differences between biological conditions.

Raw mass spectrometry data was directly submitted to Phenyx with iTRAQ 8-plex option selected for peptides/proteins identification. Details on search parameters, protein quantitation and statistical analysis could be found elsewhere [10].

Curation and analysis of the genome-scale metabolic model of *S. solfataricus* P2

Model curation and constraint-based modelling was performed as described previously [10]. For the sake of conservative estimation, active transporters (ABC-type or secondary active transporters) were chosen over passive transporters for compounds that are known to be taken up or exported by the organism when there was no detailed data available.

For the simulation of growth on D-glucose or caseinhydrolysate as sole carbon sources the uptake of carbonaceous compounds was restricted to zero $mmol \cdot g_{CDW} \cdot h^{-1}$ with the exception of CO_2, D-glucose or amino acids that were experimentally observed to be taken up. The uptake rate of D-glucose was restricted to the previously observed value of 1.13 $mmol \cdot g_{CDW} \cdot h^{-1}$ [10]. The uptake rates of individual amino acids were restricted to the maximum of the experimentally observed uptake rates. The biomass reaction *Biomass* or *Biomass_caseinhydrolysate* was used as objective function, depending on which carbon source was available in each scenario. For simulated growth on caseinhydrolysate the growth-associated maintenance energy (GAM) as well as the non-growth-associated maintenance energy (NGAM) were calculated as previously described [25], resulting in a GAM value of 28.94 mmol $ATP \cdot g_{CDW}$ and a NGAM value of 0.80 mmol $ATP \cdot g_{CDW} \cdot h^{-1}$. Here, the NGAM was fitted to the experimentally observed growth rate.

In addition to a freely optimised scenario for simulated growth on caseinhydrolysate we also defined a scenario for growth on caseinhydrolysate in which classical degradation pathways for the amino acids isoleucine and phenylalanine have been deactivated, thus forcing the model to employ oxidative Stickland reactions for degradation of these amino acids (Stickland-forced scenario).

Acknowledgements

We thank Sabine Kaltenhäuser and Steffen Lippold for technical assistance and Dr. Christopher Bräsen for carefully reading and commenting the manuscript. This work was performed within the e:Bio initiative of the Federal Ministry of Education and Research (BMBF), Germany. The following authors acknowledge the BMBF for financial support: JW and HS (0316188B), AA (0316188D). MNS and JDH were funded by the Federal State of Lower Saxony, Niedersächsisches Vorab (VWZN2889/3215). TKP and PCW acknowledge the EPSRC (EP/1031812/1) and the BBSRC (BB/M018172/1) for financial support.

Author Contributions

Conceived and designed the experiments: HS, JW, DS, MNS, JK, BS, PCW

Performed the experiments: JW, MNS, JDH, AA, TKP

Computational modelling: HS

Analysed the data: HS, JW, AA, MNS, JDH , TKP

Wrote the manuscript: HS, JW, MNS, AA, TKP with input from DS, BS, JK, PCW

References

1 Rosa MD, Gambacorta A & Bu'lock JD (1975) Extremely Thermophilic Acidophilic Bacteria Convergent with *Sulfolobus Acidocaldarius*. *J. Gen. Microbiol.* **86**, 156–164.

2 Zillig W, Stetter KO, Wunderl S, Schulz W, Priess H & Scholz I (1980) The *Sulfolobus-"Caldariella"* group: Taxonomy on the basis of the structure of DNA-dependent RNA polymerases. *Arch. Microbiol.* **125**, 259–269.

3 Nicolaus B, Trincone A, Lama L, Romano I, Marsiglia F & Gambacorta A (1991) Adaptation of *Sulfolobus solfataricus* on minimal media. *Biotechnol. Lett.* **13**, 667–670.

4 Izzo V, Notomista E, Picardi A, Pennacchio F & Di Donato A (2005) The thermophilic archaeon *Sulfolobus solfataricus* is able to grow on phenol. *Res. Microbiol.* **156**, 677–689.

5 Rosa MD, Gambacorta A, Nicolaus B, Giardina P, Poerio E & Buonocore V (1984) Glucose metabolism in the extreme thermoacidophilic archaebacterium *Sulfolobus solfataricus*. *Biochem. J.* **224**, 407–414.

6 Lamble HJ, Heyer NI, Bull SD, Hough DW & Danson MJ (2003) Metabolic Pathway Promiscuity in the Archaeon Sulfolobus solfataricus Revealed by Studies on Glucose Dehydrogenase and 2-Keto-3-deoxygluconate Aldolase. *J. Biol. Chem.* **278**, 34066–34072.

7 Grogan DW (1989) Phenotypic characterization of the archaebacterial genus *Sulfolobus*: comparison of five wild-type strains. *J. Bacteriol.* **171**, 6710–6719.

8 Brouns SJJ, Walther J, Snijders APL, Werken HJG van de, Willemen HLDM, Worm P, Vos MGJ de, Andersson A, Lundgren M, Mazon HFM, Heuvel RHH van den, Nilsson P, Salmon L, Vos WM de, Wright

PC, Bernander R & Oost J van der (2006) Identification of the Missing Links in Prokaryotic Pentose Oxidation Pathways EVIDENCE FOR ENZYME RECRUITMENT. *J. Biol. Chem.* **281**, 27378–27388.

9 Nunn CEM, Johnsen U, Schönheit P, Fuhrer T, Sauer U, Hough DW & Danson MJ (2010) Metabolism of Pentose Sugars in the Hyperthermophilic Archaea *Sulfolobus solfataricus* and *Sulfolobus acidocaldarius*. *J. Biol. Chem.* **285**, 33701–33709.

10 Wolf J, Stark H, Fafenrot K, Albersmeier A, Pham TK, Müller KB, Meyer B, Hoffmann L, Shen L, Albaum SP, Kouril T, Schmidt-Hohagen K, Neumann-Schaal M, Bräsen C, Kalinowski J, Wright PC, Albers S-V, Schomburg D & Siebers B (2016) A systems biology approach reveals major metabolic changes in the thermoacidophilic archaeon *Sulfolobus solfataricus* in response to the carbon source L-fucose versus D-glucose. *Mol. Microbiol.* **102**, 882–908.

11 Radianingtyas H & Wright PC (2003) 2-Propanol degradation by *Sulfolobus solfataricus*. *Biotechnol. Lett.* **25**, 579–583.

12 Chong PK, Burja AM, Radianingtyas H, Fazeli A & Wright PC (2007) Proteome Analysis of *Sulfolobus solfataricus* P2 Propanol Metabolism. *J. Proteome Res.* **6**, 1430–1439.

13 Limauro D, Cannio R, Fiorentino G, Rossi M & Bartolucci S (2001) Identification and molecular characterization of an endoglucanase gene, *celS*, from the extremely thermophilic archaeon *Sulfolobus solfataricus*. *Extremophiles* **5**, 213–219.

14 Park CB & Lee SB (2000) Effects of exogenous compatible solutes on growth of the hyperthermophilic archaeon *Sulfolobus solfataricus*. *J. Biosci. Bioeng.* **89**, 318–322.

15 Brock TD, Brock KM, Belly RT & Weiss RL (1972) *Sulfolobus*: A new genus of sulfur-oxidizing bacteria living at low pH and high temperature. *Arch. Für Mikrobiol.* **84**, 54–68.

16 Yokooji Y, Sato T, Fujiwara S, Imanaka T & Atomi H (2013) Genetic examination of initial amino acid oxidation and glutamate catabolism in the hyperthermophilic archaeon *Thermococcus kodakarensis*. *J. Bacteriol.* **195**, 1940–1948.

17 Heider J, Mai X & Adams MW (1996) Characterization of 2-ketoisovalerate ferredoxin oxidoreductase, a new and reversible coenzyme A-dependent enzyme involved in peptide fermentation by hyperthermophilic archaea. *J. Bacteriol.* **178**, 780–787.

18 She Q, Singh RK, Confalonieri F, Zivanovic Y, Allard G, Awayez MJ, Christina C-Y, Clausen IG, Curtis BA & De Moors A (2001) The complete genome of the crenarchaeon *Sulfolobus solfataricus* P2. *Proc. Natl. Acad. Sci.* **98**, 7835–7840.

19 Wilson H & Cannan RK (1937) The Glutamic Acid-Pyrrolidonecarboxylic Acid System. *J. Biol. Chem.* **119**, 309–331.

20 Park CB, Ryu DD. & Lee SB (2003) Inhibitory effect of l-pyroglutamate on extremophiles: correlation with growth temperature and pH. *FEMS Microbiol. Lett.* **221**, 187–190.

21 Barker HA (1981) Amino Acid Degradation by Anaerobic Bacteria. *Annu. Rev. Biochem.* **50**, 23–40.

22 Nisman B (1954) THE STICKLAND REACTION. *Bacteriol. Rev.* **18**, 16–42.

23 Stickland LH (1934) Studies in the metabolism of the strict anaerobes (genus *Clostridium*). *Biochem. J.* **28**, 1746–1759.

24 Mai X & Adams MW (1996) Purification and characterization of two reversible and ADP-dependent acetyl coenzyme A synthetases from the hyperthermophilic archaeon *Pyrococcus furiosus*. *J. Bacteriol.* **178**, 5897–5903.

25 Ulas T, Riemer SA, Zaparty M, Siebers B & Schomburg D (2012) Genome-Scale Reconstruction and Analysis of the Metabolic Network in the Hyperthermophilic Archaeon *Sulfolobus Solfataricus*. *PLoS ONE* **7**, e43401.

26 Alexander B, Leach S & Ingledew WJ (1987) The Relationship between Chemiosmotic Parameters and Sensitivity to Anions and Organic Acids in the Acidophile *Thiobacillus Ferrooxidans*. *Microbiology* **133**, 1171–1179.

27 Baker-Austin C & Dopson M (2007) Life in acid: pH homeostasis in acidophiles. *Trends Microbiol.* **15**, 165–171.

28 Park CB, Lee SB & Ryu DDY (2001) l-Pyroglutamate Spontaneously Formed from l-Glutamate Inhibits Growth of the Hyperthermophilic Archaeon *Sulfolobus solfataricus*. *Appl. Environ. Microbiol.* **67**, 3650–3654.

29 Ciaramella M, Napoli A & Rossi M (2005) Another extreme genome: how to live at pH 0. *Trends Microbiol.* **13**, 49–51.

30 Kishimoto N, Inagaki K, Sugio T & Tano T (1990) Growth inhibition of *Acidiphilium* species by organic acids contained in yeast extract. *J. Ferment. Bioeng.* **70**, 7–10.

31 Simon G, Walther J, Zabeti N, Combet-Blanc Y, Auria R, Oost JVD & Casalot L (2009) Effect of O_2 concentrations on *Sulfolobus solfataricus* P2. *FEMS Microbiol. Lett.* **299**, 255–260.

32 Russell JB & Cook GM (1995) Energetics of bacterial growth: balance of anabolic and catabolic reactions. *Microbiol. Rev.* **59**, 48–62.

33 Argüelles JC Physiological roles of trehalose in bacteria and yeasts: a comparative analysis. *Arch. Microbiol.* **174**, 217–224.

34 Nishimura H, Azami Y, Miyagawa M, Hashimoto C, Yoshimura T & Hemmi H (2013) Biochemical evidence supporting the presence of the classical mevalonate pathway in the thermoacidophilic archaeon Sulfolobus solfataricus. *J. Biochem. (Tokyo)* **153**, 415–420.

35 Kim J, Hetzel M, Boiangiu CD & Buckel W (2004) Dehydration of (R)-2-hydroxyacyl-CoA to enoyl-CoA in the fermentation of α-amino acids by anaerobic bacteria. *FEMS Microbiol. Rev.* **28**, 455–468.

36 Horner DS, Hirt RP & Embley TM (1999) A single eubacterial origin of eukaryotic pyruvate: ferredoxin oxidoreductase genes: implications for the evolution of anaerobic eukaryotes. *Mol. Biol. Evol.* **16**, 1280–1291.

37 Kletzin A & Adams MW (1996) Molecular and phylogenetic characterization of pyruvate and 2-ketoisovalerate ferredoxin oxidoreductases from *Pyrococcus furiosus* and pyruvate ferredoxin oxidoreductase from *Thermotoga maritima*. *J. Bacteriol.* **178**, 248–257.

38 Yan Z, Maruyama A, Arakawa T, Fushinobu S & Wakagi T (2016) Crystal structures of archaeal 2-oxoacid:ferredoxin oxidoreductases from Sulfolobus tokodaii. *Sci. Rep.* **6**, 33061.

39 Schut GJ, Menon AL & Adams MWW (2001) 2-keto acid oxidoreductases from *Pyrococcus furiosus* and *Thennococcus litoralis*. In (Enzymology B-M in, ed), pp. 144–158. Academic Press.

40 Awano T, Wilming A, Tomita H, Yokooji Y, Fukui T, Imanaka T & Atomi H (2014) Characterization of two members among the five ADP-forming acyl coenzyme A (Acyl-CoA) synthetases reveals the presence of a 2-(Imidazol-4-yl)acetyl-CoA synthetase in *Thermococcus kodakarensis*. *J. Bacteriol.* **196**, 140–147.

41 Bräsen C & Schönheit P (2004) Unusual ADP-forming acetyl-coenzyme A synthetases from the mesophilic halophilic euryarchaeon *Haloarcula marismortui* and from the hyperthermophilic

crenarchaeon *Pyrobaculum aerophilum*. *Arch. Microbiol.* **182**, 277–287.

42 Glasemacher J, Bock A-K, Schmid R & Schönheit P (1997) Purification and Properties of Acetyl-CoA Synthetase (ADP-forming), an Archaeal Enzyme of Acetate Formation and ATP Synthesis, from the Hyperthermophile *Pyrococcus furiosus*. *Eur. J. Biochem.* **244**, 561–567.

43 Schönheit P, Buckel W & Martin WF (2016) On the Origin of Heterotrophy. *Trends Microbiol.* **24**, 12–25.

44 Siddiqui MA, Fujiwara S, Takagi M & Imanaka T (1998) In vitro heat effect on heterooligomeric subunit assembly of thermostable indolepyruvate ferredoxin oxidoreductase. *FEBS Lett.* **434**, 372–376.

45 Luengo JM, Arias S, Arcos M & Olivera ER (2007) The Catabolism of Phenylacetic Acid and Other Related Molecules in *Pseudomonas putida* U. In *Pseudomonas* (Ramos J-L & Filloux A, eds), pp. 147–192. Springer Netherlands.

46 Teufel R, Mascaraque V, Ismail W, Voss M, Perera J, Eisenreich W, Haehnel W & Fuchs G (2010) Bacterial phenylalanine and phenylacetate catabolic pathway revealed. *Proc. Natl. Acad. Sci.* **107**, 14390–14395.

47 Kennedy SP, Ng WV, Salzberg SL, Hood L & DasSarma S (2001) Understanding the Adaptation of *Halobacterium* Species NRC-1 to Its Extreme Environment through Computational Analysis of Its Genome Sequence. *Genome Res.* **11**, 1641–1650.

48 Chang A, Schomburg I, Placzek S, Jeske L, Ulbrich M, Xiao M, Sensen CW & Schomburg D (2014) BRENDA in 2015: exciting developments in its 25th year of existence. *Nucleic Acids Res.*, gku1068.

49 Schäfer T & Schönheit P (1991) Pyruvate metabolism of the hyperthermophilic archaebacterium Pyrococcus furiosus. *Arch. Microbiol.* **155**, 366–377.

50 Altschul SF, Madden TL, Schäffer AA, Zhang J, Zhang Z, Miller W & Lipman DJ (1997) Gapped BLAST and PSI-BLAST: a new generation of protein database search programs. *Nucleic Acids Res.* **25**, 3389–3402.

51 Schäfer G, Engelhard M & Müller V (1999) Bioenergetics of the Archaea. *Microbiol. Mol. Biol. Rev.* **63**, 570–620.

52 Wolstencroft K, Owen S, du Preez F, Krebs O, Mueller W, Goble C & Snoep JL (2011) The SEEK: A Platform for Sharing Data and Models in Systems Biology. In *Methods in Enzymology* (Daniel Jameson MV and HVW, ed), pp. 629–655. Academic Press.

53 Consalvi V, Chiaraluce R, Politi L, Gambacorta A, De ROSA M & Scandurra R (1991) Glutamate dehydrogenase from the thermoacidophilic archaebacterium *Sulfolobus solfataricus*. *Eur. J. Biochem.* **196**, 459–467.

54 Schinkinger MF, Redl B & Stöffler G (1991) Purification and properties of an extreme thermostable glutamate dehydrogenase from the archaebacterium *Sulfolobus solfataricus*. *Biochim. Biophys. Acta BBA - Gen. Subj.* **1073**, 142–148.

55 Marino G, Nitti G, Arnone MI, Sannia G, Gambacorta A & Rosa MD (1988) Purification and characterization of aspartate aminotransferase from the thermoacidophilic archaebacterium *Sulfolobus solfataricus*. *J. Biol. Chem.* **263**, 12305–12309.

56 Jain S, Caforio A & Driessen AJM (2014) Biosynthesis of archaeal membrane ether lipids. *Microb. Physiol. Metab.* **5**, 641.

57 Buckel W (2001) Unusual enzymes involved in five pathways of glutamate fermentation. *Appl.*

Microbiol. Biotechnol. **57**, 263–273.

58 Neumann-Schaal M, Hofmann JD, Will SE & Schomburg D (2015) Time-resolved amino acid uptake of *Clostridium difficile* 630Δerm and concomitant fermentation product and toxin formation. *BMC Microbiol.* **15**, 281.

59 Zaparty M, Esser D, Gertig S, Haferkamp P, Kouril T, Manica A, Pham TK, Reimann J, Schreiber K, Sierocinski P, Teichmann D, Wolferen M van, Jan M von, Wieloch P, Albers SV, Driessen AJM, Klenk H-P, Schleper C, Schomburg D, Oost J van der, Wright PC & Siebers B (2010) "Hot standards" for the thermoacidophilic archaeon *Sulfolobus solfataricus*. *Extremophiles* **14**, 119–142.

60 Guida M, Salvatore MM & Salvatore F (2015) A Strategy for GC/MS Quantification of Polar Compounds via their Silylated Surrogates: Silylation and Quantification of Biological Amino Acids. *J. Anal. Bioanal. Tech.*

61 Trautwein K, Will SE, Hulsch R, Maschmann U, Wiegmann K, Hensler M, Michael V, Ruppersberg H, Wünsch D, Feenders C, Neumann-Schaal M, Kaltenhäuser S, Ulbrich M, Schmidt-Hohagen K, Blasius B, Petersen J, Schomburg D & Rabus R (2016) Native plasmids restrict growth of *Phaeobacter inhibens* DSM 17395: Energetic costs of plasmids assessed by quantitative physiological analyses. *Environ. Microbiol.* **18**, 4817–4829.

62 Macpherson HT & Slater JS (1959) γ-Amino-*n*-butyric, aspartic, glutamic and pyrrolidonecarboxylic acid; their determination and occurrence in grass during conservation. *Biochem. J.* **71**, 654–660.

63 Hottes AK, Meewan M, Yang D, Arana N, Romero P, McAdams HH & Stephens C (2004) Transcriptional Profiling of *Caulobacter crescentus* during Growth on Complex and Minimal Media. *J. Bacteriol.* **186**, 1448–1461.

64 Anders S & Huber W (2010) Differential expression analysis for sequence count data. *Genome Biol.* **11**, R106.

65 Mooser D, Maneg O, Corvey C, Steiner T, Malatesta F, Karas M, Soulimane T & Ludwig B (2005) A four-subunit cytochrome bc_1 complex complements the respiratory chain of *Thermus thermophilus*. *Biochim. Biophys. Acta BBA - Bioenerg.* **1708**, 262–274.

Tables

Table 1: **Overview of the 50 most differentially expressed genes and differentially produced proteins with known or postulated annotation in *S. solfataricus* P2 after growth on caseinhydrolysate.** Genes and proteins which were not significantly changed but discussed in the text are also included. Transcripts and proteins were identified from RNASeq (Transcriptome) and iTRAQ (Proteome) analysis. The fold change represents the relative abundance of every gene or protein averaged from three independent experiments. Cells of *S. solfataricus* P2 grown on glucose were used as reference. All cultures were harvested in the late exponential growth phase to ensure comparability between the different conditions. Each locus was assigned to one of the following categories if possible: transport processes (Transport), amino acid biosynthesis (Biosynthesis) or amino acid degradation (Degradation).
[a] Fold change in relative abundance as compared to the D-glucose reference condition.
[b] p-value < 0.01 (transcriptomics) or < $2.6 \cdot 10^{-2}$ (proteomics) indicates statistically significant differential expression.
[c] not determined.

Locus tag	EC class	Product	Category	Trancriptome		Proteome	
				Fold change[a]	p-value[b]	Fold change[a]	p-value[b]
Sso1351		Permease, multidrug efflux	Transport	34.05	5.2E-52	ND[c]	
Sso1352		Transcriptional regulator, marR family, putative		25.21	2.0E-11	ND[c]	
Sso2704		Permease, multidrug efflux	Transport	24.30	3.1E-45	ND[c]	
Sso1907	1.4.1.3	NAD specific glutamate dehydrogenase (gdhA-2)	Degradation	22.01	1.3E-43	9.93	3.4E-05
Sso1162		Multidrug resistance protein	Transport	18.63	3.9E-39	ND[c]	
Sso11071	1.2.7.-	Ferredoxin oxidoreductase subunit delta	Degradation	17.33	4.4E-06	ND[c]	
Sso2087	3.1.1.-	Carboxylesterase / Dienelactone hydrolase	Degradation	17.03	5.6E-36	4.30	2.3E-03
Sso2044	1.4.1.3	NAD specific glutamate dehydrogenase (gdhA-4)	Degradation	15.78	2.2E-37	9.19	2.5E-05
Sso2824		Predicted molibdopterin-dependent oxidoreductase YjgC		15.64	3.3E-36	13.64	1.9E-04
Sso1742		Terminal quinol oxidase, subunit (doxD)		14.85	1.4E-09	ND[c]	
Sso1817	2.8.1.1	Thiosulfate sulfurtransferase (cysA-2)		14.58	3.1E-32	7.52	5.1E-05
Sso2757	1.2.7.-	Ferredoxin oxidoreductase subunit alpha	Degradation	14.54	1.2E-08	ND[c]	
Sso8687		Partial transposase ISC1190		14.35	1.0E-04	ND[c]	
Sso2758	1.2.7.-	Ferredoxin oxidoreductase subunit gamma	Degradation	14.29	1.2E-13	ND[c]	
Sso1209		Putative oxidoreductase molybdopterin-binding subunit		11.86	8.9E-15	14.01	1.1E-04
Sso2756	1.2.7.-	Ferredoxin oxidoreductase subunit beta	Degradation	13.43	3.0E-32	ND[c]	
Sso1127		Heterodisulfide reductase, subunit C (hdrC-1)		13.34	5.4E-32	12.90	1.1E-03
Sso1741		Terminal quinol oxidase, subunit II (doxA)		12.10	9.4E-09	ND[c]	

Sso2647		ABC transporter, ATP binding protein	Transport	11.07	1.5E-28	ND[c]	
Sso1131		Heterodisulfide reductase, subunit A (hdrA)		8.98	1.5E-25	4.31	1.7E-02
Sso1183		Inorganic phosphate transporter	Transport	8.54	3.0E-20	ND[c]	
Sso1134		Heterodisulfide reductase subunit C (hdrC-2)		8.19	2.4E-21	3.69	9.7E-03
Sso2079		DPSL-type antioxidant enzyme		8.13	3.6E-22	ND[c]	
Sso2701		Permease, major facilitator superfamily	Transport	8.04	1.3E-08	ND[c]	
Sso1135		Heterodisulfide reductase, subunit B (hdrB-2)		7.89	2.0E-21	ND[c]	
Sso1123	1.8.1.4	Dihydrolipoamide dehydrogenase (pdhD-1)		7.73	2.6E-21	ND[c]	
Sso0786		Amino acid specific permease	Transport	7.51	1.0E-19	ND[c]	
Sso2821		FDHD protein homolog (fdhD)		7.08	1.7E-11	ND[c]	
Sso3211	2.6.1.19	4-aminobutyrate aminotransferase (gabT-2)	Degradation	5.11	1.1E-14	7.04	2.4E-04
Sso1184	3.3.2.1	Isochorismatase related protein (entB-like1)		6.79	2.0E-20	ND[c]	
Sso1580		Molybdopterin oxidoreductase, molybdopterin binding subunit		6.77	1.9E-18	ND[c]	
Sso1906		Amino acid transporter related protein	Transport	0.14	1.2E-05	ND[c]	
Sso2069	1.2.7.8	Indolepyruvate ferredoxin oxidoreductase beta subunit (iorB)	Degradation	3.38	6.4E-08	ND[c]	
Sso2067	1.2.7.8	Indolepyruvate ferredoxin oxidoreductase alpha subunit (iorA)	Degradation	3.36	8.9E-09	ND[c]	
Sso1806		Putative acetate-CoA ligase	Degradation	1.60	3.0E-02	2.23	3.3E-02
Sso0527	2.7.2.3	Phosphoglycerate kinase		1.59	1.5E-01	2.62	1.3E-04
Sso2053	1.14.14.9	4-hydroxyphenylacetate-3-hydroxylase (hpaA)		1.40	2.0E-01	ND[c]	
Sso0528	1.2.1.12	Glyceraldehyde-3-phosphate dehydrogenase (GAPDH)		1.06	7.7E-01	1.34	4.6E-02
Sso3042	1.1.1.47	Glucose 1-dehydrogenase (dhg-2)		0.44	3.6E-04	ND[c]	
Sso3003	1.1.1.47	Glucose 1-dehydrogenase (dhg-1)		0.37	3.5E-06	0.40	3.0E-04
Sso2970		Quinol oxidase-2, cytochrome b (soxG)		0.14	8.0E-07	ND[c]	
Sso2043		Amino acid transporter related protein	Transport	0.14	7.1E-09	ND[c]	
Sso3069		Arabinose ABC transporter, ATP-binding protein	Transport	0.21	1.7E-12	0.14	1.7E-03
Sso2971		Quinol oxidase-2, rieske iron-sulfur protein-2 (soxF)		0.14	4.0E-06	ND[c]	
Sso0876	2.7.2.4	Aspartokinase (akH)	Biosynthesis	0.23	2.4E-03	0.13	8.8E-06
Sso3060	3.2.1.51	Alpha-fucosidase C-terminal fragment (fucA1)		0.13	2.8E-04	ND[c]	

Sso2505		Sugar transport protein	Transport	0.12	2.6E-19	ND[c]	
Sso0579	2.2.1.6	Acetolactate synthase large subunit homolog (ilvB-2)	Biosynthesis	0.12	2.8E-24	0.17	6.3E-03
Sso3051	3.2.1.20	Alpha-glucosidase (malA)		0.11	2.5E-24	ND[c]	
Sso2972		Quinol oxidase-2, sulfocyanin (blue copper protein) (soxE)		0.10	1.5E-04	ND[c]	
Sso0905	1.1.1.95	3-phosphoglycerate dehydrogenase (serA-1)	Biosynthesis	0.10	4.0E-27	0.39	9.6E-03
Sso1333	4.1.3.1	Isocitrate lyase (aceA/icl)		0.09	3.0E-30	0.09	1.2E-05
Sso1054		Ammonium transporter	Transport	0.09	6.3E-05	ND[c]	
Sso0977	2.3.3.13	2-isopropylmalate synthase (leuA-2)	Biosynthesis	0.07	3.8E-03	0.06	5.5E-04
Sso0127	2.3.3.13	2-isopropylmalate synthase, putative (leuA-1)	Biosynthesis	0.05	3.7E-41	ND[c]	
Sso0683		Glutamate synthase domain 1; Conserved hypothetical protein	Biosynthesis	0.04	1.2E-13	ND[c]	
Sso0503		Predicted metal permease	Transport	0.03	4.0E-14	ND[c]	
Sso0684	1.4.1.13	Glutamate synthase (NADPH) subunit alpha (gltB)	Biosynthesis	0.01	5.4E-44	ND[c]	

Table 2: Identified intracellular metabolites that were only detected in cells of *S. solfataricus* P2 grown on either caseinhydrolysate or glucose as sole carbon source. All cultures were harvested in the late exponential growth phase with 15 mg cell dry weight for each sample, to ensure comparability between the two conditions.

Caseinhydrolysate	Glucose
2-Amino-2-methyl-3-hydroxypropanoate	α-D-Galactopyranosyl-(1,4)-D-galactopyranoside
2-Hydroxyphenylacetate	β-Alanine
2-Keto-3-deoxygluconate	1-O-methyl-α-galactopyranoside
2,3-Dehydroadipyl-CoA	2-Methylmalate
3-Methyl-2-butenoyl-CoA	2-Pentenoyl-CoA
3-Oxo-5,6-dehydrosuberyl-CoA semialdehyde	Benzoyl-CoA
3,4-Dihydroxybenzoate	Erythritol
4-Hydroxybenzoate	Erythronic acid
4-Methylthio-2-oxobutanoate	Hexanoyl-CoA
Alanine	Nicotinic acid
Butyro-1,4-lactam	Xylitol
Homoserine	Xylulose

Lysine	
Methionine	
N-acetyl-putrescine	
Norspermidine	
Phenylacetate	
Pipecolate	
Proline	
Spermidine	
Tyrosine	

Table 3: Amino acid uptake rates and degradation pathways in the metabolic model.
Growth on medium containing caseinhydrolysate was simulated using the parameters detailed in the methods sections. Amino acids that were not taken up are not listed. Relative fluxes below 0.5 % are not shown.
[1] Maximum uptake rates of individual amino acids were experimentally determined during the logarithmic growth phase. The observed peak areas for individual amino acids at start of cultivation were considered to equal 100%. These relative values were set off against the absolute concentration of amino acids in the medium [58]. Averages of the maximal observed uptake rates were used for metabolic modelling.
[2] Missing relative amounts are consumed in the biomass reaction. When multiple pathways are mentioned in a single row, the relative fraction has been cumulated from these pathways.
[3] Freely optimised scenario without restraints concerning amino acid degradation pathways that voluntarily uses oxidative Stickland reactions for degradation of leucine and tyrosine.
[4] Scenario with forced oxidative Stickland reactions: Common pathways for degradation of branched-chain or aromatic amino acids have been deactivated, thus forcing the model to use oxidative Stickland reactions wherever possible, including the amino acids isoleucine and phenylalanine.
[5] Biomass precursors such as amino acids and nucleotides are not listed.

Amino acid	**Uptake rate[1] [µmol·g_{CDW}^{-1}·h^{-1}]**	**Degradation via pathway**	**Predicted fraction[2] of amino acid in scenario [%]**		**Product(s)[5]**
			free[3]	**forced[4]**	
Alanine	42.1 ± 2.1	Transamination using 2-oxoglutarate as nitrogen acceptor	75.8	78.7	Pyruvate
Aspartate	44.7 ± 4.5	Transamination using 2-oxoglutarate as nitrogen acceptor	22.2	31.4	Oxaloacetate
		Asparagine biosynthesis	20.0	17.6	
		Arginine biosynthesis	19.9	17.5	
		Nucleotide biosynthesis	18.7	16.5	

Glutamate	241.8 ± 10.8	Deamination via glutamate dehydrogenase	62.7	68.0	2-Oxoglutarate
		Transamination for biosynthesis of arginine, glutamine, valine, serine, glycine, cysteine and lysine	34.2	29.4	2-Oxoglutarate
Glycine	6.7 ± 0.5	Nucleotide biosynthesis	21.2	21.2	
Isoleucine	28.1 ± 1.4	Common degradation pathway	38.7	-	Succinyl-CoA
		Oxidative Stickland reactions	-	46.0	2-Methylbutanoate
Leucine	76.1 ± 3.3	Oxidative Stickland reactions	49.0	55.0	3-Methyl-2-butenoate
		Conversion to mevalonate for isoprenoid biosynthesis	26.4	23.3	
Methionine	21.6 ± 0.9	Degradation via subsequent formation of cystathionine and 2-oxobutanoate	72.5	75.7	Propanoyl-CoA
		Biosynthesis of cobalamin, sulfolobusquinone and polyamines via formation of S-adenosyl-L-methionine	9.7	8.6	
Phenylalanine	21.9 ± 1.0	Degradation via common bacterial degradation pathway [46]	63.6	-	2 equivalents acetyl-CoA 1 equivalent succinyl-CoA
		Oxidative Stickland reactions	-	67.9	2-Hydroxyphenylacetate
Threonine	19.7 ± 0.9	Degradation via formation of 2-oxobutanoate	56.2	61.4	Propanoyl-CoA
		Cobalamin biosynthesis	1.0	0.9	
Tyrosine	11.4 ± 0.6	Oxidative Stickland reactions	20.8	30.2	4-Hydroxyphenylacetate

Table 4: Comparison of ATP-contributing pathways in the metabolic model.
Growth on medium containing caseinhydrolysate was simulated using the parameters detailed in the methods sections. The contribution of different pathways towards the total metabolite flux of ATP in the metabolic model was calculated for two different scenarios. Included in these values is the production of reduced electron carriers (like NADH) which can subsequently be used for production of ATP during respiration.
[1] Scenario without restraints concerning amino acid degradation pathways that voluntarily uses oxidative Stickland reactions for degradation of leucine and tyrosine.
[2] Scenario with forced oxidative Stickland reactions: Common pathways for degradation of branched-chain or aromatic amino acids have been deactivated, thus forcing the model to use oxidative Stickland reactions wherever possible, including the amino acids isoleucine and phenylalanine.

Pathway	Total ATP production in scenario [%]	
	free[1]	forced[2]
TCA cycle	72.0	68.9
Amino acid degradation excluding oxidative Stickland reactions	15.2	17.1
Pyruvate decarboxylation	6.6	7.1
Oxidative Stickland reactions	2.8	3.2

Table 5: Global changes in transcriptome, proteome and metabolome of *S. solfataricus* grown on caseinhydrolysate.
Cells grown on glucose were used as reference.
* p-values < 0.01 (transcriptomics, metabolomics) or < $2.6 \cdot 10^{-2}$ (proteomics) indicate a statistically significant increase. For transcriptomics also a minimum fold-change of 4 was expected for a statistically significant increase in transcript levels.

Technique	Detection scope	Identification scope	Significantly* changed loci / metabolites	
			Increased	Decreased
Transcriptomics	7.8 to 15.3 million reads	37.4% – 69.7% mapped reads	66	99
Proteomics	5240 peptides	580 proteins	35	40
Metabolomics	93 compounds	74 metabolites	50	25

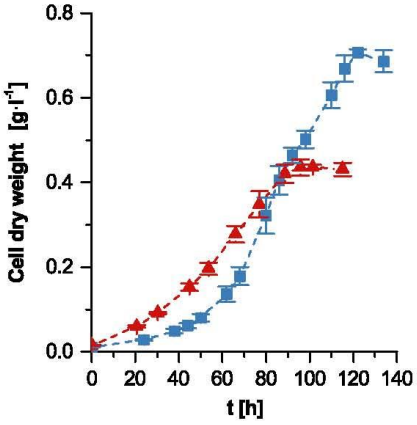

Figure 1: Growth curve of *S. solfataricus* P2.
The organism was cultivated on defined media, containing either 1 % (w/v) caseinhydrolysate (▲) or 0.44 % (w/v) glucose (■) as carbon source. The cell dry weight was calculated from measured optical densities. All values represent the average of three biological replicates. Error bars represent the standard deviation between the experiments.

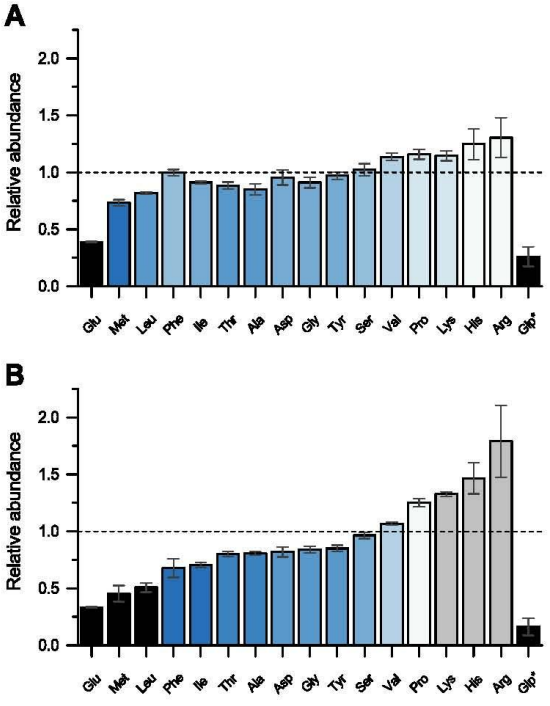

Figure 2: Amino acid depletion profile of *S. solfataricus* P2 on caseinhydrolysate containing medium at different growth stages.

The organism was cultivated on defined medium, containing 1 % caseinhydrolysate as carbon and nitrogen source. The time-resolved amino acid consumption profile of 16 detectable amino acids as well as pyroglutamate (Glp) in cell free culture supernatants is shown for (A) the exponential growth phase at 66 hours of cultivation and (B) for the end of cultivation at 101 hours. The relative abundance is expressed as compared to the available amount at the beginning of cultivation (time point 0). All values represent the average of three biological replicates. Error bars represent the standard deviation between the experiments.

* The relative abundance of pyroglutamate (Glp) is expressed as compared to the available amount of glutamate at the beginning of cultivation as Glp was not present at the start of cultivation.

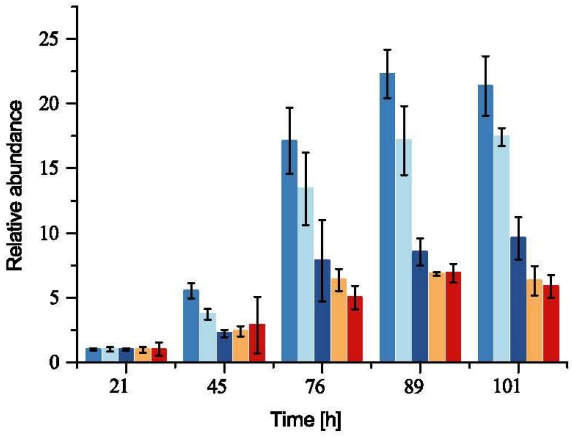

Figure 3: Secretion of branched-chain organic acids by *S. solfataricus* P2 on caseinhydrolysate containing medium.

All compounds start to appear in the media after 21 h of cultivation, hence this value was used as the reference time point to determine the relative abundances of isovalerate (■), 2-methyl-2-butenoate (■), 3-methyl-2-butenoate (■), 2-methylbutanoate (■) and isobutanoate (■). After 101 h the compounds accumulated to the following absolute concentrations [mM]: isovalerate (2.44 ± 0.26), 2-methylbutanoate (0.46 ± 0.08), isobutanoate (0.42 ± 0.06), 2-methyl-2-butenoate (0.13 ± 0.01) and 3-methyl-2-butenoate (0.03 ± 0.01). All values represent the average of three biological replicates. Error bars represent the standard deviation between the experiments.

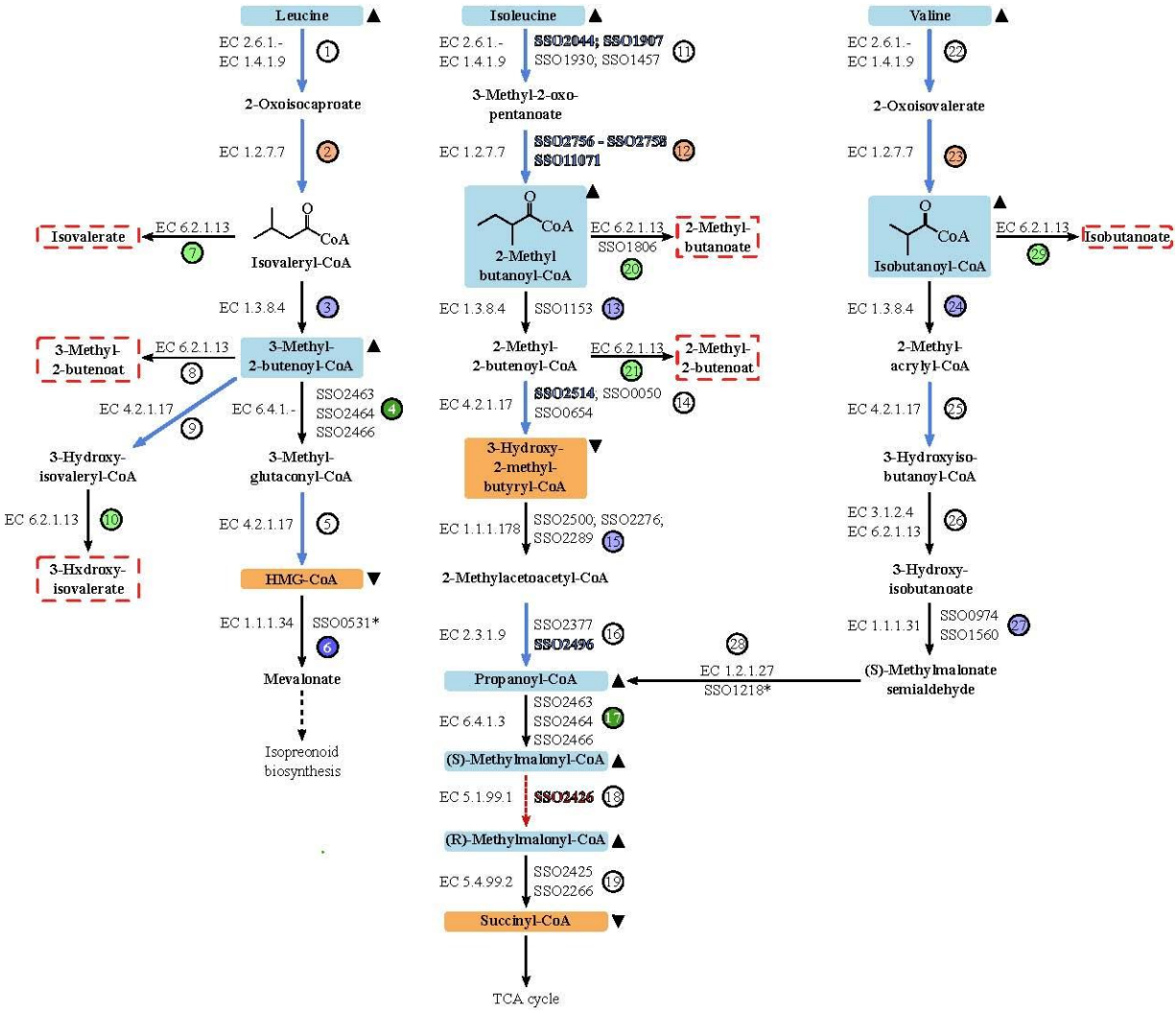

Figure 4: Overview of the reconstructed branched-chain amino acid catabolism in *S. solfataricus* P2.
Protein functions were predicted using the metabolic model as well as EnzymeDetector and BLAST-based annotations. Reactions with the same EC-number are suggested to be catalysed by the same set of enzymes, so that the corresponding gene loci are only indicated once. Metabolites were detected in the intracellular (closed rectangles) or extracellular (dashed red rectangles) space. Changes in the intracellular metabolite abundance of cells grown on caseinhydrolysate against a glucose reference are indicated by symbols and node colour (■ / ▲ increased abundance; ■ / ▼ decreased abundance). Significant regulation of genes or gene products is indicated by both arrow and font colour as well as arrow style (blue solid arrow: up-regulated; red dotted arrow: down-regulated). Reactions are numbered in order to facilitate discussion in text. The reaction numbers are coloured in order to signal the production (black font) or consumption (white font) of the cofactors ATP (green background), NAD(P)H (blue background) and reduced ferredoxins (orange background).
Abbreviations: HMG-CoA: 3-Hydroxy-3-methylglutaryl-CoA.
* Proven protein function

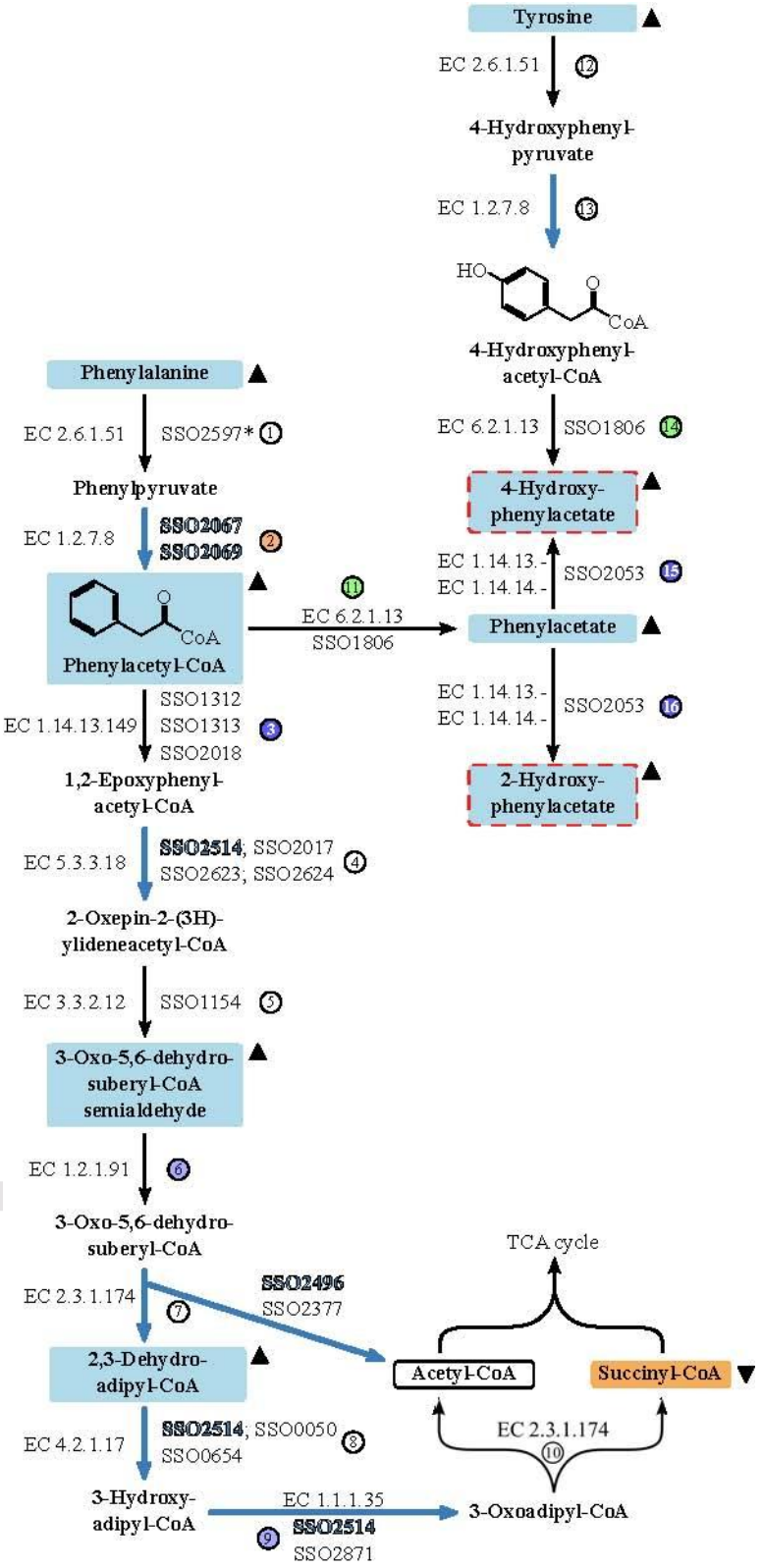

Figure 5: Reconstruction of aromatic amino acid metabolism in *S. solfataricus* P2.
Protein functions were predicted using the metabolic model as well as EnzymeDetector and BLAST-based annotations. Reactions with the same EC-number are suggested to be catalysed by the same set of enzymes, so that the corresponding gene loci are only indicated once. Metabolites were detected in the intracellular (closed rectangles) or extracellular (dashed red rectangles) space. Changes in the intracellular metabolite abundance of cells grown on caseinhydrolysate against a glucose reference are indicated by symbols and node colour (■ / ▲ increased abundance; ■ / ▼ decreased abundance). Significant Significant regulation of genes or gene products is indicated by both arrow and font colour as well as arrow style (blue solid arrow: up-regulated; red dotted arrow: down-regulated). Reactions are numbered in order to facilitate discussion in text. The reaction numbers are coloured in order to signal the production (black font) or consumption (white font) of the cofactors ATP (green background), NAD(P)H (blue background) and reduced ferredoxins (orange background).
* Proven protein function

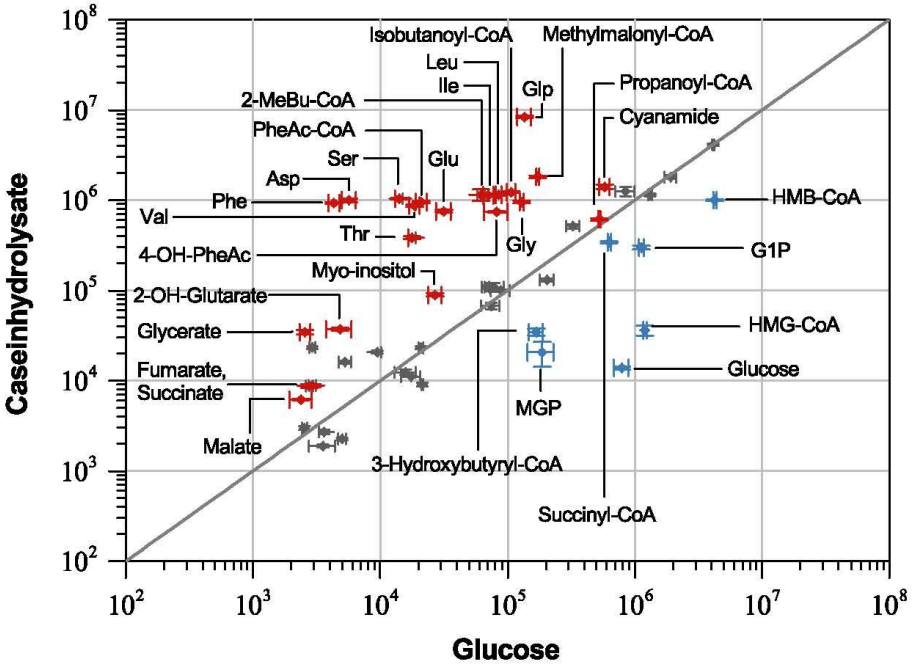

Figure 6: Intracellularly detected metabolites in *S. solfataricus* P2 grown with either caseinhydrolysate or D-glucose as carbon source.

Normalised peak areas were plotted on a double logarithmic scale. Red: more abundant in cells grown on caseinhydrolysate blue: more abundant in cells grown on glucose, grey: unchanged. Note that only identified metabolites with significantly altered abundances (Benjamini-Yekutieli corrected Kruskal-Wallis test, p-value < 0.01) are labelled. Values represent the average of three independent experiments. Error bars represent the standard error between the three experiments.

Abbreviations: 2-MeBu-CoA: 2-Methylbutanoyl-CoA; G1P: Glycerol-1-phosphate*; HMB-CoA: 3-Hydroxy-2-methylbutyryl-CoA; HMG-CoA: 3-Hydroxy-3-methylglutaryl-CoA; MGP: Methyl-α-D-glucopyranoside; 2-OH-glutarate: 2-Hydroxyglutarate; 4-OH-PheAc: 4-Hydroxyphenylacetate; PheAc-CoA: Phenylacetyl-CoA; Glp: Pyroglutamate.

*Glycerol-1-phosphate is identified as glycerol-3-phosphate by GC-MS analysis, however, this method can not distinguish between the two metabolites and glycerol-3-phosphate is not part of the organism's metabolism.